Ultramicroscopy 160 (2016) 252–255

Contents lists available at ScienceDirect

Ultramicroscopy

journal homepage: www.elsevier.com/locate/ultramic

Full length article

Theoretical estimates of spherical and chromatic aberration in photoemission electron microscopy

J.P.S. Fitzgerald *, R.C. Word, R. Könenkamp

Portland State University, Department of Physics, PO Box 751, Portland, OR 97207, United States

ARTICLE INFO

Article history:
Received 5 March 2015
Received in revised form
28 September 2015
Accepted 29 October 2015
Available online 30 October 2015

Keywords:
Photoemission electron microscopy
PEEM
Electron optics
Spherical aberration
Chromatic aberration
Aberration correction

ABSTRACT

We present theoretical estimates of the mean coefficients of spherical and chromatic aberration for low energy photoemission electron microscopy (PEEM). Using simple analytic models, we find that the aberration coefficients depend primarily on the difference between the photon energy and the photoemission threshold, as expected. However, the shape of the photoelectron spectral distribution impacts the coefficients by up to 30%. These estimates should allow more precise correction of aberration in PEEM in experimental situations where the aberration coefficients and precise electron energy distribution cannot be readily measured.

Photoemission electron microscopy (PEEM) is an increasingly effective method for imaging surfaces and surface near-field processes in the ultraviolet, visible, and infrared spectral regions [1–3]. High peak intensity pulsed lasers allow practical imaging of nonlinear two- and three-photon photoelectron excitations on femtosecond time scales [4–7]. Moreover, with monochromatic and coherent light sources, PEEM permits the observation of optical diffraction and interference with high spatial resolution, and this in turn has opened the way for the quantitative study of photonic and plasmonic processes in the visible and infrared [8–14]. These developments make PEEM a powerful tool for the study of near-field optics, offering both excellent spatial resolution and ultrafast time resolution.

Spherical and chromatic aberration strongly limit spatial resolution in PEEM. Simultaneous correction of spherical and chromatic aberration is possible through the use of electrostatic mirrors [15–19]. However, in PEEM there is currently no direct method to fully characterize the aberration coefficients, which makes the design and operation of aberration correcting optics subject to uncertainty. This situation is qualitatively different from other electron microscopies, where the electron beam aberration can be quantitatively determined for a given sample to allow subsequent correction [18,19]. In PEEM the aberration coefficients depend sensitively on the energy distribution of the photoelectrons, which can have significant width and structure that depends on the difference between emission threshold energy and photon energy. Here we present a method for the estimation of spherical and chromatic aberration coefficients in PEEM from the accelerating potential, cathode-to-anode distance, and emission energy distribution of the photoelectrons. Furthermore, we investigate the uncertainty in these estimates when the precise energy distribution shape is unknown using simple geometric models motivated by realistic spectra [20–31].

Spherical and chromatic aberrations in PEEM primarily originate in the accelerating field and objective lens [32–36]. Here we consider the aberrations of the accelerating field only. The aberration coefficients of subsequent lenses depend on the lay-out of the instrument and are comparatively insensitive to the emission energy maximum and distribution. However, a complete accounting of image aberration requires the magnifications and aberrations of the objective and other lenses. In particular, the spherical aberration of the objective lens can be as large as that of the accelerating field. For the purpose of this paper, the lens properties can be separately measured or computed, and then they can be added to the accelerating field aberrations following the method of Rempfer [33,35,37–39]. This method includes the effects of the accelerating field anode aperture.

We focus on the emission energy region near threshold, which is relevant to ultraviolet and multi-photon PEEM. The virtual specimen position of the accelerating field can be computed from simple kinematic arguments [33,35]. Retaining only the leading

* Corresponding author.
E-mail address: fit@pdx.edu (J.P.S. Fitzgerald).

http://dx.doi.org/10.1016/j.ultramic.2015.10.023
0304-3991/

order contribution in V_e/V_a, the virtual specimen is located a distance

$$z_a = 2\ell_a\left(1 - \sqrt{V_e/V_a}\cos\alpha_e\right) \tag{1}$$

behind the anode, where ℓ_a is the distance between the sample plane (cathode) and the anode at potential V_a, α_e is the photoelectron emission angle relative to the surface normal, and eV_e is the photoelectron emission energy. The paraxial virtual specimen position is

$$z_{a,0} = 2\ell_a\left(1 - \sqrt{V_e/V_a}\right). \tag{2}$$

The virtual specimen position varies with electron trajectory angle and energy. As a result, the image possesses both spherical and chromatic aberrations.

Chromatic aberration requires careful treatment, so we begin with the definition of the longitudinal chromatic aberration of the accelerating field,

$$\Delta_e z_{a,0} = \langle z_{a,0}\rangle - z_{a,0}(V_e), \tag{3}$$

where $\langle z_{a,0}\rangle$ is the mean position of the paraxial virtual specimen. The mean position is calculated from an energy-weighted average,

$$\langle z_{a,0}\rangle = \int_0^{V_{e,\max}} z_{a,0}(V_e)\rho(V_e)\,dV_e, \tag{4}$$

where the electron charge e has been dropped for convenience, $\rho(V_e)$ is the emission energy distribution, and integration is over the full emission energy spectrum $(0, V_{e,\max}]$. The energy distribution is equal-yield normalized such that

$$\int_0^{V_{e,\max}} \rho(V_e)\,dV_e = 1. \tag{5}$$

The lowest rank coefficient of chromatic aberration can be defined by

$$z_{a,0} - \langle z_{a,0}\rangle = C_{ca}\left(\frac{\langle V_e\rangle - V_e}{\langle V_e\rangle}\right) + O(\alpha, \delta V_e^2), \tag{6}$$

where $O(\alpha, \delta V_e^2)$ represents higher order dependence with angle and energy.

Next we consider the meaning of $\langle V_e\rangle$ in Eq. (6) in order to derive a simple expression for C_{ca}. Typically, $e\langle V_e\rangle$ is taken to be the mean emission energy, i.e., derived from $\bar{V}_e = \int V_e\,\rho(V_e)\,dV_e$. However, this interpretation presents some difficulty since $\langle z_{a,0}\rangle \neq z_{a,0}(\bar{V}_e)$, i.e., the mean position of the virtual specimen is not the same as the position for the mean energy. As a result, the left-hand and right-hand sides of Eq. (6) are equal at slightly different energies. To remedy this discrepancy, we define $\langle V_e\rangle$ as the energy of the mean position. Explicitly, if we equate Eqs. (2) and (4), we get the expression

$$\langle V_e\rangle = V_a\left(1 - \langle z_{a,0}\rangle/2\ell_a\right)^2. \tag{7}$$

Using this definition, we arrive at the simple and familiar result for the lowest order coefficient of chromatic aberration [32],

$$\langle C_{ca}\rangle = -\ell_a\sqrt{V_a/\langle V_e\rangle}. \tag{8}$$

Calculations made with this result agree with those using a direct series expansion of Eq. (6) if and only if $\langle V_e\rangle$ is defined by Eq. (7). A similar approach also yields the mean coefficient of spherical aberration [32,36],

$$\langle C_{sa}\rangle = \ell_a\sqrt{V_a/\langle V_e\rangle} = -\langle C_{ca}\rangle. \tag{9}$$

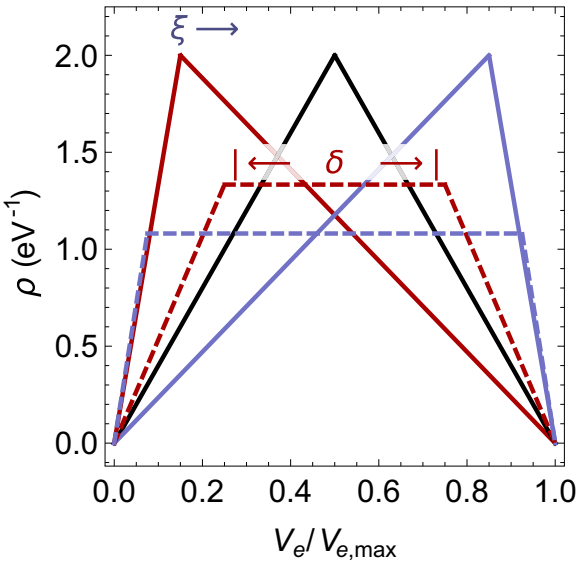

Fig. 1. Simple equal-yield distributions to investigate the effects of asymmetry and width on the coefficients of spherical and chromatic aberration. The triangle distribution $\rho_\triangle$ (solid lines) varies the relative position ξ of the maximum. The symmetric trapezoid distribution $\rho_\square$ (dashed lines) varies the relative width δ of the central region. The two distributions are equal when ξ=0.5 and δ=0 (solid black line). (For interpretation of the references to color in this figure caption, the reader is referred to the web version of this paper.)

Since the expressions for virtual specimen position and the aberration coefficients vary with emission energy, the mean values $\langle z_{a,0}\rangle$, $\langle C_{sa}\rangle$, and $\langle C_{ca}\rangle$ in general depend on the distribution of emission energies. Typically, the distribution is assumed to be a simple step or truncated Gaussian function in electron optics. In this case, the maximum energy of the distribution $eV_{e,\max} \approx nh\nu - \phi$ largely determines the values of $\langle C_{sa}\rangle$ and $\langle C_{ca}\rangle$, where ϕ is the photoemission threshold energy, and $nh\nu$ is the energy of the n photons required to liberate an electron. The distribution of real electron emission energies is often complicated, especially for multi-photon emission. Spectra can exhibit one or more asymmetrically shaped peaks of varying widths depending on the photon energy, material and surface conditions [20–31]. Indeed, these deviations are usually considered desirable features that reveal the internal electronic structure of materials. In these cases, the shape of the distribution $\rho(V_e)$ is also important since C_{sa} and C_{ca} are nonlinear with factors of $\langle V_e\rangle$ in the denominator.

For our purposes, we make the broad simplification that the overall distribution can be described as an irregular triangle or trapezoid as shown in Fig. 1. First, the triangular model is used to investigate the effects of an asymmetric spectrum as a function of $\xi = V_{e,0}/V_{e,\max} \in (0, 1)$, where $V_{e,0}$ is the energy at the maximum of the distribution. Similarly, the symmetric trapezoid model is used to investigate the effects of distribution width, where $\delta \in (0, 1)$ is the relative width of the trapezoid top at maximum emission. Thus, the triangular distribution $\rho_\triangle$ with ξ=0.5 is the same as the trapezoid distribution $\rho_\square$ with δ=0. The simplicity of these models offers analytic expressions for the coefficients of spherical and chromatic aberration of the accelerating field. In particular, the triangular distribution yields a compact expression for the mean coefficient of spherical aberration,

$$\langle C_{sa}\rangle_\triangle = \frac{15}{8}\ell_a\sqrt{\frac{V_a}{V_{e,\max}}}\left(\frac{1-\xi}{1-\xi^{3/2}}\right), \tag{10}$$

Explicit definitions of the distribution functions and derivations of